Fermilab

TM-1088
1183.000
July, 1982

Activation of the Major Constituents of Tissue and Air by a Fast Neutron Radiation Therapy Beam.

Randall K. Ten Haken, Miguel Awschalom, Ivan Rosenberg

ABSTRACT

The production of ^{11}C, ^{13}N, ^{15}O from C, N, O, and of ^{39}Cl and ^{41}Ar from Ar by a p(66)Be(49) clinical neutron therapy beam has been measured. The results of these measurements were used to estimate the production of other radionuclides, then to estimate airborne radioactivity in a typical neutron therapy room and radioactivity induced in body tissues during treatment.

Only under special circumstances would airborne radioactivity necessitate a waiting period before entering a typical treatment room. The additional dose to a treatment volume due to decay products from radioactivity induced within that volume would amount to a few thousandths of the given dose and the additional body dose outside the treated volume would be a few millionths of the given dose.

INTRODUCTION

Modern neutron therapy beams, generated by 40 to 70 MeV protons incident on semithick beryllium targets,[1] have spectra with neutron energies reaching to within a couple of MeV of the incident proton energy. These neutrons produce radionuclides through activation of collimators, air, patient tissues and any equipment in or near the neutron beam, which may pose radiation problems for attending personnel.[2,3] Results of measurements of radioactivity produced in the most common tissue and air resident elements by a p(66)Be(49)[a] neutron therapy beam are reported in this work. Applications of the results are also discussed.

Since C, N and O are the major constituents of both tissues and air this report concentrates on the creation of ^{11}C, ^{13}N, and ^{15}O, principally via (n,2n) reactions. These positron emitters are easily detected by their annihilation radiation and they have half-lives which make their production easy. The (n,2n) cross sections in C, N, and O are characterized by a 10-20 MeV threshold and maximum cross-sectional values of approximately 10-30 mb.[4,5] The cross section for $^{12}C(n,2n)$ calculated by Dimbylow[6] is presented as an example (Fig. 1). The p(66)Be(49) neutron therapy beam at Fermilab[7-10] was used in this study. An estimate[11] of its neutron energy spectrum is given in Fig. 2. More than half of the total neutron flux in the p(66)Be reference beam and more than a

third of that for the p(41)Be reference beam are above the 10-20 MeV threshold (Fig. 2).

The production of ^{41}Ar and ^{39}Cl through activation of Ar was also investigated. High energy neutrons in the same range as those above are required for production of ^{39}Cl [via $^{40}Ar(p,pn)$ and $^{40}Ar(p,d)$], whereas low energy neutrons are more important for ^{41}Ar production [via $^{40}Ar(n,\gamma)$].

Other radionuclides are also produced by neutron bombardment of C, N, O, and Ar. Of special importance are ^{16}N, and ^{12}B, However, their short half-lives (7.13 s and .0204 s, respectively) make measurements difficult. Consequently, only estimates of their production rates were made and used below.

MEASUREMENTS

Small samples of graphite, melamine ($C_3H_6N_6$), distilled water and argon gas were irradiated in the neutron beam at 190 cm from the target. After activation, the samples were transferred to another vessel for counting in either a 10.2 cm X 12.7 cm NaI(Tl) well counter or by a Ge(Li) detector.

The decay of positron activity from the graphite, melamine and water samples was measured as a function of time with a well counter system connected to a multichannel scaler. Counts from the entire 0.511 MeV γ-ray annihiliation radiation spectrum (singles and coincidence) and just the 1.022 MeV sum peak were recorded on two separate systems. Data was collected using either 10 s or 20 s dwell times. Background rates were also noted for each measurement and three to five measurements were made with each compound. The mass of each sample was determined through use of a precision balance. The efficiencies of the well counter system were determined in separate experiments with activated samples of water and polyethylene using the "sum-peak method."[13-15] Corrections due to incomplete solid angle coverage[15,16] were minimized by using small samples. The measured total efficiency, $\varepsilon = 0.749 \pm 0.022$, and the 0.511 MeV photo peak efficiency, $\varepsilon_p = .479 \pm .024$ compare well with calculated values for detectors of similar geometry.[17]

A Ge(Li) multichannel spectrometer system was used for the argon measurements. Balloons filled with the gas were irradiated in the neutron beam and then transferred to another balloon for counting. Gamma rays originating in the decay of ^{41}Ar and ^{39}Cl were identified. The measured efficiencies[18] were corrected for the finite geometry of the balloon. The mass of argon was estimated from the balloon volume and pressure.

DATA REDUCTION

The decay data for the graphite, melamine and distilled water measurements were corrected for dead time on a channel by channel basis and fitted by a function consisting of a series of exponentials plus a flat background using a non-linear least squares fitting routine.[19,20] The known half-lives [$\tau(1/2)$] of the positron emitters and the measured background were used as input. The number of decays in the initial counting interval was determined for each sample from data for the whole spectrum as well as for just the 1.022 MeV sum peak. All data were fitted with chi-squares per degree of freedom between 1.0 and 1.3.

The graphite data (Fig. 3) are fitted quite adequately with a single decay curve corresponding to production of ^{11}C [$\tau(1/2)$ = 20.4 min] plus background. The presence of other decay products was not detected.

The melamine ($C_3H_6N_6$) decay data (Fig. 4) are well described by the decay of ^{13}N [$\tau(1/2)$ = 9.96 min] and ^{11}C. The fit to the data was not improved by including decay products other than ^{11}C and ^{13}N.

The distilled water data (Fig. 5) are best fitted by the decay of three nuclides; ^{11}C, ^{13}N, and ^{15}O [$\tau(1/2)$ = 2.03 min]. Fits to the data become markedly worse if either the ^{13}N or ^{11}C term is omitted and no improvement in fit is obtained by trying to include another term in the description. (In particular, γ-ray contributions to the total spectrum from the decay of ^{16}N [$\tau(1/2)$ = 7.13 s] were not observed, due to typical lag times of several minutes between activation and counting.) This detection of ^{11}C and ^{13}N is discussed below.

The argon decay data were analyzed by hand for the production of ^{41}Ar[$\tau(1/2)$=1.83 hr] and ^{39}Cl[$\tau(1/2)$=56.2 min]. Background subtracted peak values were obtained for each 10-20 minute counting interval. The number of decays in the first counting interval was computed by linear regression analysis using known half lives and a small correction term for gas leakage. Other reaction products are certainly present, but, due to the longer lag times involved here (20 - 30 min), signals from shorter lived products were not seen, and peaks with much lower yields were not analyzed.

ANALYSIS AND RESULTS

The usual equations[21] relating production and decay were used to compute the production rates of transformed nuclei per parent nucleus normalized, for convenience, to proton current I_p incident on the neutron producing target. We write:

$$\frac{\sigma\phi}{I_p} = \frac{A(t_A+t_L)}{N_o \text{ eff } [1-\exp(-\lambda t_A)] \exp(-\lambda t_L)} \cdot \frac{1}{I_p} , \qquad (1)$$

where σ represents the production cross section, ϕ the incident neutron fluence rate, λ the decay constant of interest, t_A the production time and t_L the lag time before counting. The activity $A(t_A + t_L)$ was obtained from fits to the data described above. The number of parent nuclei N_o was computed from the measured masses of the samples using known elemental compositions. The efficiency term eff is equal to $(\varepsilon_p)^2$ for the 1.022 MeV sum peak, $\varepsilon(2-\varepsilon)$ for the total singles plus coincidence spectrum and the measured efficiency multiplied by a geometry correction term for the Ge(Li) peaks.

The results are summarized in Table 1. Values are weighted averages of all runs taken for each nuclide. Individual results were weighted by the inverse square of their statistical uncertainty. The errors quoted represent standard deviations of

the means. The sum peak and total spectrum results for O, N, and C agreed quite well with each other and were all included in the averages. An extra scale factor uncertainty of two is associated with the argon results due to imprecise determination of the gas mass.

The presence of ^{13}N and ^{11}C from activation of oxygen follows directly from the distilled water data reduction and curve fitting discussed above. The ^{15}O component is certainly expected. On the other hand, (n, 2n) reactions involving realistic quantities of dissolved gases cannot even begin to explain the amount of ^{11}C and ^{13}N observed. The production of significant quantities of ^{13}N from $^{16}O(p,\alpha)$ initiated by protons emitted from neutron reactions with the hydrogen and oxygen in water has been previously observed.[22,23] Calculations based on published cross sections[4,5,24,25] and on yields obtained here indicate that this (p,α) mechanism accounts for a large portion of the observed ^{13}N (and of the excess ^{11}C from activation of melamine observed below). Ratios of yields are consistent with those reported from activation of H_2O (and NH_4NO_3) by a lower energy neutron beam at Hammersmith.[23] Higher energy neutrons and protons are apparently also initiating spallation-type reactions on oxygen leading to the production of some ^{11}C and ^{13}N. The magnitudes of cross sections reported for reactions initiated by 50 MeV protons[26,27] support such an assumption.

The presence of ^{11}C from activation of nitrogen in melamine (Table 1) is based on the graphite results. The ^{11}C signal from melamine is too large to be associated with reactions involving carbon only. The graphite results were used with Eq. 1 to compute the expected amount of ^{11}C from activation of the carbon in melamine. Subtraction of that value from the total ^{11}C signal leads to the stated value of ^{11}C production from activation of nitrogen. The excess ^{11}C signal is attributed to contributions from $^{14}N(p,\alpha)$ from knock-on protons and N-spallation as discussed above.

Comparison of published fast neutron cross sections for production of ^{39}Cl and ^{41}Ar from activation of argon[28] to the yields observed here (Table 1) indicates that the vast majority of ^{41}Ar activity is not associated with fast neutrons. This is not surprising in light of argon's large thermal cross section.[28] The thermal flux from room scattered neutrons was not measured here and the amount of low energy neutrons present in the primary beam is uncertain.[11] Hence, the value presented here for production of ^{41}Ar is specific to the conditions under which is was measured. Thermal neutron fluxes will change as phantom, room materials and irradiation conditions are changed.

The values in Table 1 are all that is needed, in conjunction with elemental compositions, to compute the majority of the activity produced from neutron bombardment of the C, N, O, and Ar

present in air and tissue. The production rates of other shorter lived and/or less abundant nuclides may be estimated by comparison of the energy dependence and magnitude of published cross sections and then scaling the values listed in Table 1 accordingly. Two applications of these results follow.

ACTIVATION OF AIR

Activation of air around proton and electron accelerator facilities has been studied extensively in the past.[29-38] At least three reports[36-38] have dealt directly with air transmutation in a medical setting. The activation of air by therapeutic neutron beams has not been widely addressed, although it could be a possible source of exposure to personnel.

Following the nomenclature of Kase,[31] we assume uniform irradiation of an air volume V with uniform dispersal of radioactivity in a room volume P which has a ventilation rate Q. Activity builds up as

$$\frac{dN}{dt} = \sigma\phi N_o - \lambda N - (Q/P)N \ . \qquad (2)$$

The number of transformed nuclei present after bombardment time t_A is

$$N(t_A) = \frac{\sigma\phi n_o V}{(\lambda+Q/P)}\{1-\exp[-(\lambda+Q/P)t_A]\} , \quad (3)$$

where n_o represents the number of target nuclei per unit volume. The activity $A(t_A) = \lambda N(t_A)$ has a concentration $C(t_A) = A(t_A)/P$ and decays as $\exp[(-\lambda+ Q/P)t]$.

Using Table 1 values and the elemental composition of dry air at STP[39] (75.5% N, 23.2% O, 1.3% Ar, ρ = 1.293 kg m^{-3}) we may compute the specific activity of each radioactive product at saturation ($t_A = \infty$, $Q = 0$) per unit incident proton current on target, $\sigma\phi n_o/I_p$ (Table 2). Values listed represent the total induced activity summed over all constituents of air. The ^{16}N value is an estimate based on comparison of the (n,p) and (n,2n) cross sections on ^{16}O.[28] Predominant species are ^{13}N, ^{15}O, ^{11}C and ^{16}N. The study of radioactive gas production by electron beams[31,34,36-38] has generally concentrated on ^{13}N and ^{15}O. ^{41}Ar production has also been estimated to be important in proton accelerator facilities.[30,32]

The times required for each nuclide to reach equilibrium (exponential term in Eq. 3 equal to 0.01)[31] in any room for different levels of ventilation may be computed (Table 3). With the exception of ^{16}N, all times are quite long compared to standard treatment times and equilibrium will rarely be attained except during prolonged dosimetry or radiobiology irradiations.

As a specific numerical example, we considered an unattenuated trapezoidal beam volume of total length 5 m defining a 30 x 30 cm^2 field at 170 cm from the source, a room volume of 200 m^3 and an incident proton current of 100 μA. Under conditions where equilibrium has been reached, we computed the equilibrium concentrations for the various radionuclides (Table 4). We note that shorter-lived nuclides become relatively more important for larger ventilation rates. Maximum permissible concentrations in air $(MPC)_a$ for most of the nuclides listed above have been calculated by various authors[30,31,36,40,41] using methods outlined in ICRP 2[42], taking either the whole body or skin as the limiting organ. Values range from .37 to 2.96 MBq m^{-3} (1 to 8 x 10^{-5} μCi cm^{-3}). Taking a limiting composite $(MPC)_a$ of .37 MBq m^{-3} (10^{-5} μCi cm^{-3}) for the sum of all species, we see that at equilibrium the total concentration of radioactivity exceeds safe limits. The post-bombardment time necessary for this sum of equilibrium concentrations to decay to our composite $(MAC)_a$ can be computed noting that individual nuclides decay at their own characteristic rates in the calculation. These waiting times are listed at the bottom of Table 4 along with waiting times necessary for a reduction of I_pV/P by a factor of two.

In practice, equilibrium is rarely achieved, ventilation rates are typically 6 - 8 air changes per hour, and the time necessary to access the room may be 0.2 - 0.5 minutes. Thus, in the example given above, air activation is just marginally a

problem that may rarely require waiting time. For p(41)Be neutron beams (Fig. 2), approximately one quarter as many neutrons per unit incident proton current have energies above the threshold for (n,2n) reactions and air activation should be of little concern, although, due to lower yields[43,44] than p(66)Be, either incident particle currents and/or treatment times will be larger.

ACTIVATION OF TISSUE

Radioactivity induced in various tissues by photons,[45-49] protons,[50,51] and neutrons[52,53] has long been of interest as a source of added patient dose,[45,47,50] as a means of monitoring the concentration of some element *in vivo* [46,49,50,52,53] or for assessing dose distributions.[48,51]

We assume a sample whose composition is an average of the total soft tissue and total skeleton values listed by Constantinou[54] from reference man[55] (10.00% H, 23.24% C, 2.70% N, 60.83% O, 0.14% Na, 0.02% Mg, 1.11% P, 0.20% S, 0.12% Cl, 0.20% K and 1.43% Ca by weight with a density of 1.07 g cm^{-3}).

For a static situation in which all induced activity decays where it was formed, the total number of transformed nuclei of a species produced in an activation time t_A is $N(t_A) = \sigma\phi n_o V t_A$. Using this, the elemental composition above and the data in Table

1, we computed radionuclide production rates per unit volume normalized to incident proton current, $\sigma\phi n_o/I_p$, and the specific activities per unit dose, $(\sigma\phi/I_p)n_o\lambda(\dot{D}/I_p)^{-1}$ (Table 5). $\dot{D}/I_p$ is the dose rate per unit proton current, taken here as 3.2×10^{-4} Gy $s^{-1}\mu A^{-1}$, the value at d_{max} for our p(66)Be(49) beam with a 10 x 10 cm^2 field at 170 cm SAD. Values for ^{12}B and ^{16}N were estimated from comparison of (n,2n) and (n,p) cross sections on C and O, respectively.[28] Order of magnitude estimates for other isotopes (^{28}Al, ^{30}P, ^{31}Si and ^{32}P from ^{31}P; ^{24}Na from ^{23}Na; ^{34}Cl from ^{35}Cl; ^{38}K from ^{39}K; ^{42}K from ^{41}K; and ^{49}Ca from ^{48}Ca) were also made from comparison of fast and thermal neutron cross sections[28] and our measured yields. As mentioned earlier, results from comparison of thermal values are specific to the unmeasured thermal neutron flux present during our argon measurements. Contributions to added dose from the listed radionuclides, however, are found to be relatively unimportant and they are not discussed separately here.

The dose corresponding to the total decay of the induced activity may be obtained for each nuclide using a standard expression[56] such as

$$D(Gy) = 1.6 \times 10^{-13} \frac{A}{\lambda}\{\overline{E}_\beta/m + \sum f_\gamma E_\gamma \Phi_\gamma\} \qquad (4)$$

where A is the total activity (Bq), λ is the decay constant (s^{-1}), $\bar{E}_\beta$(MeV) is the average positron or electron energy, m(kg) is the mass of tissue absorbing the dose, f_γ is the fraction of decays resulting in a gamma ray of energy E (MeV) and Φ_γ is the specific absorbed fraction of E_γ in m. The summation is carried out over all the emitted photon energies.

For illustration, we consider one liter of centrally located average tissue uniformly irradiated to a dose of 1 Gy under the dose rate conditions described above. Using the data in Table 5 and Eq. 4 we calculated the dose added to that irradiated volume, the dose added to the whole body, and the γ-dose added to the whole body not in the irradiated volume. Half-lives, electron, positron and gamma ray energies and γ-ray abundances were obtained from the Table of the Isotopes.[57] Average electron and positron energies were estimated using a standard approximation.[58] Values of Φ_γ used were averages for activity concentrated in centrally located organs of mass similar to that of the irradiated volume.[55] The results are summarized in Table 6. The largest portion of the added dose is predicted to come from decay of ^{16}N and ^{11}B, (results derived from production rate estimates) with doses from the positron decay of ^{11}C, ^{13}N and ^{15}O being the only other processes of importance. The additional dose added locally, 3 x 10^{-3} Gy, is an insignificant part of the total treatment dose. The total body dose (including β-decays) and the body γ-dose outside the treatment volume of 6 x 10^{-5} and 7 x 10^{-6} Gy per

target absorbed Gy, respectively, are quite small. They should not pose a problem in neutron therapy where scattered neutron and photon doses outside the treatment volume are expected to be much larger.[59,60] The total body burdens listed, however, are 5-50 times greater than those predicted by Standen for photon activation of tissue elements.[47]

SUMMARY AND CONCLUSIONS

Measurements of ^{11}C, ^{13}N, ^{15}O, ^{39}Cl and ^{41}Ar production rates from activation of C, N, O, and Ar by a p(66)Be(49) neutron beam have been presented. Estimates of the production rates of other radionuclides, principally ^{16}N and ^{11}B, have also been made by comparison of published neutron cross sections to the measurements. A direct measurement of ^{16}N and ^{11}B activity would be useful due to the magnitude of their projected production rates.

The results have been applied to activation of air in a typical treatment room and to activation of tissue during treatment. Both computations indicate only minimal reason for concern from a radiation protection viewpoint.

ACKNOWLEDGMENT

This investigation was supported by PHS Grant Number 5P01CA18081-08, awarded by the National Cancer Institute, DHHS. The authors also wish to thank Dr. Sam Baker and Mr. Jay Baldwin of the Fermilab Radiation Safety Department for their assistance, the unknown referees for their editorial suggestions and Miss Michelle Gleason for typing this manuscript with fortitude and patience.

REFERENCES

(a) The expression p(66)Be(49) means that 66 MeV protons are incident on a semi-thick target, where protons not undergoing nuclear scattering lose 49 MeV by ionization. p(66)Be would mean a thick target.

1. L. Cohen and M. Awschalom, "Fast Neutron Radiation Therapy", Ann. Rev. Biophys. Bioeng. 11, 359 (1982).

2. I. Rosenberg, M. Awschalom, R. K. Ten Haken and B. R. Bennett, Analysis of Personnel Exposures in Neutron Therapy Facilities, Accepted for publication, Health Phys. (1983).

3. J. Eenmaa, I. Kalet, R. Risler and P. Wootton, The University of Washington Clinical Neutron Therapy Facility, Med. Phys. 9, 620 (1982). (Abstract)

4. O. D. Brill, N. A. Vlasov, S. P. Kalinin and L. S. Sokolov, "Cross Section of the (n,2n) Reaction in ^{12}C, ^{14}N, ^{16}O, and ^{19}F in the Energy Interval 10-37 MeV", Doklady Akademii Nauk SSSR 136 (1961) 55; English translation Sov. Phys.-Dokl. 6, 24 (1961).

5. W. G. Davey, R. W. Goin and J. R. Ross, "Analysis of (n,2n) Cross-section Measurements for Nuclei up to Mass 238", Argonne National Lab. report ANL-75-34, Available from National Technical Information Service, Springfield, VA (1975).

6. P. J. Dimbylow, Proceedings of International Conference on Neutron Physics and Neutron Data for Reactors and Other Applied Purposes, the National Radiological Protection Board, Harwell, England, 636 (1978).

7. I. Rosenberg and M. Awschalom, Characterization of a p(66)Be(49) Neutron Therapy Beam I: Central Axis Depth dose and Off-Axis Ratios, Med. Phys. 8, 99 (1981).

8. M. Awschalom and I. Rosenberg, Characterization of a p(66)Be(49) Neutron Therapy Beam II: Skin Sparing and Dose Transition Effects, Med. Phys. 8, 105 (1981).

9. L. Cohen and M. Awschalom, The Cancer Therapy Facility at the Fermi National Accelerator Laboratory, Batavia, Illinois. A Preliminary Report, Appl. Radiol. 5, 51 (1976).

10. M. Awschalom, L. Grumboski, A. F. Hrejsa, G. M. Lee and I. Rosenberg, The Fermilab Cancer Therapy Facility: Status Report After 2.5 Years of Operation, IEEE Trans. Nucl. Sci. NS-26, 3068 (1979).

11. M. Awschalom, I. Rosenberg and A. Mravca, "Kermas for Various Substances Averaged Over the Energy Spectra of Fast Neutron Therapy Beams", accepted for publication, Med. Phys. 10, (1983).

12. R. G. Graves, J. B. Smathers, P. R. Almond, W. H. Grant and V. A. Otte, "Neutron Energy Spectra of d(49)Be and p(41)Be Neutron Radiotherapy Sources", Med. Phys. 6, 123 (1979).

13. G. A. Brinkman, A. H. W. Aten, Jr., and J. T. Veenboer, Absolute Standardization with a NaI(Tl) Crystal-I Calibration by Means of a Single Nuclide, Int. J. Appl. Rad. Isotopes 14, 153 (1963).

14. G. A. Brinkman, A. H. W. Aten, Jr., and J. T. Veenboer, Absolute Standardization with a NaI(Tl) Crystal-II Determination of the Total Efficiency, Int. J. Appl. Rad. Isotopes 14, 433 (1963).

15. G. A. Brinkman and A. H. W. Aten, Jr., Absolute Standardization with a NaI(Tl) Crystal-III Calibration of β^+ Emitters, Int. J. Appl. Rad. Isotopes 14, 503 (1963).

16. W. Mannhart and H. Vonach, Absolute Calibration of a Well-Type NaI Detector to an Accuracy of 0.3 - 0.1%, Nucl. Instr. and Meth. 136, 109 (1976).

17. P. Holmberg, R. Rieppo and P. Passi, Calculated Efficiency Values for Well-Type NaI(Tl)-Detectors, Int. J. Appl. Rad. Isotopes 23, 115 (1972).

18. S. I. Baker, C. R. Kerns, S. H. Pordes, J. B. Cumming, A. Soukas, V. Agoritsas and G. R. Stevenson, "Absolute Cross Section for Production of ^{24}Na in Copper by 400 GeV Protons", submitted for publication Nucl. Instr. & Meth. (1983). P. O. Box 500, Batavia, IL 60510. Private communication.

19. P. R. Bevington, Data Reduction and Error Analysis for the Physical Sciences, McGraw Hill: New York (1969).

20. D. W. Marquardt, An Algorithm for Least-Squares Estimation of Nonlinear Parameters, J. Soc. Ind. Appl. Math. 11, 431 (1963).

21. R. D. Evans, The Atomic Nucleus, New York: McGraw-Hill, 470f (1955).

22. M. O. Leach, B. J. Thomas, and D. Vartsky, "Total Body Nitrogen Measured by the ^{14}N(n,2n)^{13}N Method: A Study of the Interfering Reactions and the Variation of Spatial Sensitivity with Depth", Int. J. Appl. Rad. Isotopes 28, 263 (1977).

23. T. J. Spinks, "Measurement of Body Nitrogen by Activation Analysis", Int. J. Appl. Rad. Isotopes 29, 409 (1978).

24. B. W. Wieland, R. R. Highfill and P. H. King, "Proton Accelerator Targets for the Production of ^{11}C, ^{13}N, ^{15}O and ^{18}F", IEEE Trans. Nucl. Sci., NS-26, 1713 (1979).

25. T. W. Burrows and P. Dempsey, The Bibliography of Integral Charged Particle Nuclear Data, Brookhaven National Laboratory Report BNL-NCS-50640, fourth edition, available from National Technical Information Service, Springfield, VA (1980).

26. I. G. Golikov, M. N. Zhukov, I. I. Loshchakou and B. I. Ostroumov, "Cross Sections for Reactions in ^{12}C, ^{14}N and ^{16}O Induced by 50-MeV Protons with Three Charged Particles in the Final State", Yadernaya Fizika 27, 7 (1978), English translation Sov. J. Nucl. Phys. 27, 3 (1978).

27. A. I. Vdovin, I. G. Golikov, M. N. Zhukov, I. I. Loshchakou and V. I. Ostroumov, "Cross Sections of Reactions Due to the Action of Protons Having an Energy of 50 MeV on ^{12}C, ^{14}N and ^{16}O Nuclei", Investiya Akademii Nauk SSSR, Seriya Fizicheskaya 43, 148 (1979). English translation Bull. Acad. Sci. USSR, Physical Series 43, 124 (1979).

28. D. I. Garber and R. R. Kinsey, Neutron Cross Sections Volume II, Curves, Brookhaven National Laboratory Report BNL 325, third edition, available from National Technical Information Service, Springfield, VA (1976).

29. R. H. Thomas, "Rough Estimates of Radiation Hazard from Radioactive Gas in Machine Tunnel", Health and Safety Laboratory, New York, UCID 10136, unpublished (1964).

30. A. Rindi and S. Charalambus, "Airborne - Radioactivity Produced at High-Energy Accelerators", CERN Internal Report DI/HP/80, unpublished (1966).

31. K. R. Kase, Radioactive Gas Production at a 100-MeV Electron Linac Facility, Health Phys. 13, 869 (1967).

32. M. Awschalom, F. L. Larsen and W. Schimmerling, Activation of Argon Near a Traget Irradiated by 3 GeV Protons, Health Phys. 14, 345 (1968).

33. M. Awschalom, F. L. Larsen and W. Schimmerling, Activation of air Near a Target Bombarded by 3 GeV Protons, Nucl. Instr. & Meth. 75, 93 (1969).

34. A. Brynjolfsson and T. G. Martin, III, Bremsstrahlung Production and Shielding of Static and Linear Electron Accelerators Below 50 MeV. Toxic Gas Production, Required Exhaust Rates, and Radiation Protection Instrumentation, Int. J. Appl. Rad. Isotopes 22, 29 (1971).

35. J. I. Cehn, A Study of Radioactive Airborne Effluents From Particle Accelerators, U.S. E.P.A. Report ORP/TAD-79-12, National Technical Information Services #PB80 10 1314, Springfield, VA (1979).

36. A. F. Holloway and D. V. Cormack, Radioactive and Toxic Gas Production by a Medical Electron Linear Accelerator, Health Phys. 38, 673 (1980).

37. W. L. Dorn, Zum Problem der Luftaktivierung bei der Megavolttherapie mit 15 bis 20 MeV, Strahlentherapie 156, 836 (1980).

38. H. Gremmel, E. Ihnen and J. M. Jensen, Messung und Berechnung der Luftaktivierung durch die 15-MeV-Bremsstrahlung eines Linearbeschleunigers, Strahlentherapie 157, 187 (1981).

39. ICRU Report No. 10b, Physical Aspects of Irradiation, International Commission on Radiation Units and Measurements, Washington, D. C. (1964).

40. K. R. Kase, $(MPC)_a$ for ^{13}N, Health Phys. 15, 283 (1968).

41. C. Yamaguchi, MPC Calculation for the Radionuclides Produced During Accelerator Operation, Health Phys. 29, 393 (1975).

42. ICRP Report No. 2, Report of Committee II on Permissible Dose for Internal Radiation, International Commission on Radiological Protection, New York: Pergamon Press (1959).

43. H. I. Amols, J. F. Dicello, M. Awschalom, L. Coulson, S. W. Johnsen, and R. B. Theus, "Physical Characteristics of Neutron Beams Produced by Protons and Deuterons of Various Energies Bombarding Beryllium and Lithium Targets of Several Thicknesses", Med. Phys. 4, 486 (1977).

44. R. K. Ten Haken, M. Awschalom and I. Rosenberg, "Update of Neutron Dose Yields as a Function of Energy for Protons and Deuterons Incident on Beryllium Targets", Fermilab Internal Report TM-1146 (1982).

45. M. V. Mayneord, J. H. Martin and D. A. Layne, Production of Radioactivity in Animal Tissue by High Energy X-Rays, Nature 164, 728 (1949).

46. E. Spring and T. Väyrynen, Measurement of Changes in the Oxygen and Carbon Concentration of Tissues During Fractionated High Energy X-Ray Treatment, Phys. Med. Biol. 15, 23 (1970).

47. E. Stranden, Activity Induced in Patients by High Energy X-Ray Therapy, Phys. Med. Biol. 22, 348 (1977).

48. G. W. Bennett, R. Dobert, J. Meltzer, B. E. Archambeau and J. O. Archambeau, Induced Radioactivity in Patients from Betatron Irradiation, Brit. J. Radiol. 54, 53 (1981).

49. R. K. Ten Haken, G. H. Nussbaum, B. Emami and W. L. Hughes, Photon Activation - ^{15}O Decay Studies of Tumor Blood Flow, Med. Phys. 8, 324 (1981).

50. S. Graffman and B. Jung, ^{11}C and ^{15}O Induced in the Mouse by 175 MeV Protons, Acta Radiol. Therapy Phys. Biol. 14, 113 (1975).

51. G. W. Bennett, J. O. Archambeau, B. E. Archambeau, J. I. Meltzer and C. L. Wingate, Visualization and Transport of Positron Emission from Proton Activation in vivo, Science 200, 1151 (1978).

52. H. C. Biggin and W. D. Morgan, Fast Neutron Activation Analysis of the Major Body Elements, J. Nucl. Med. 12, 808 (1971).

53. A. Sharafi, D. Pearson, C. B. Oxby, B. Oldroyd, D. W. Krupowicz, K. Brooks and R. E. Ellis, "Multi-Element Analysis of the Human Body Using Neutron Activation", Phys. Med. Biol. 28, 203 (1983).

54. C. Constantinou, Phantom Materials for Radiation Dosimetry. I. Liquids and Gels, Brit. J. Radiol. 55, 217 (1982).

55. ICRP Report No. 23, Report of the Task Group on Reference Man, International Commission on Radiological Protection, New York: Pergamon Press (1975).

56. R. Loevinger and M. Berman, A Revised Schema for Calculating the Absorbed Dose From Biologically Distributed Radionuclides, MIRD Pamphlet No 1 (Rev), New York: Society of Nuclear Medicine (1976).

57. Table of the Isotopes, 7th Edition, C. M. Lederer and V. S. Shirley Editors, New York: John Wiley & Sons (1978).

58. Handbook of Radioactive Nuclides, Y. Wang, Editor, Cleveland: Chemical Rubber Co., 172 (1969).

59. D. K. Bewley and B. C. Page, On the Nature and Significance of the Radiation Outside the Beam in Neutron Therapy, Brit. J. Radiol. 51, 375 (1978).

60. J. P. Geraci, K. L. Jackson and M. S. Mariano, "An Estimate of the Radiation-induced Cancer Risk from the Whole-body Stray Radiation Exposure in Neutron Radiotherapy", Eur. J. Cancer Clin. Oncol. 18, 1187 (1982).

Table 1

Production Rate per Parent Atom per Incident Proton

Current for a p(66)Be(49) Neutron Beam.†

TARGET	PRODUCT	HALF-LIFE (minutes)	$\frac{\sigma\phi}{I_p} = \frac{\text{Transmutations}}{\text{second}\ \mu A} \times 10^{-21}$
C	^{11}C	20.4	34.4 ± 0.7
N	^{13}N	9.96	18.4 ± 0.9
	^{11}C	20.4	3.60 ± 1.13
O	^{15}O	2.03	30.0 ± 1.6
	^{13}N	9.96	1.79 ± 0.27
	^{11}C	20.4	4.33 ± 0.37
Ar	^{41}Ar	110.	20.0 ± 7.0
	^{39}Cl	56.2	4.7 ± 2.6

† At 0° and 190 cm from the neutron production target.

Table 2

Saturation Specific Activity per Unit Proton Current Induced in Dry Air[39] at STP by Neutrons from a p(66)Be(49) Beam†

NUCLIDE	$\sigma\phi n_o I_p^{-1}$	
	kBq μA^{-1} m^{-3}	μCi μA^{-1} ℓ^{-1}
^{11}C	201 ± 47	5.44 ± 1.27 E-3
^{13}N	790 ± 38	2.14 ± 0.10 E-2
^{15}O	338 ± 18	9.12 ± 0.49 E-3
^{39}Cl	0.25 ± 0.11	6.8 ± 3.0 E-6
^{41}Ar	5.1 ± 1.8	1.4 ± 0.5 E-4
(^{16}N)*	(400 ± 270)	(1.1 ± 0.7 E-3)

† At 0° and 190 cm from the neutron production target.

*Estimate, see text.

Table 3

Production Time (minutes) Required to Reach Equilibrium

in Air Activation at Different Ventilation Rates

NUCLIDE	Air Changes Per Hour					
	0	2	4	6	8	10
^{11}C	136	68	46	34	28	23
^{13}N	66	45	34	27	23	20
^{15}O	13.6	12.4	11.4	10.5	9.8	9.1
^{39}Cl	373	101	58	41	32	26
^{41}Ar	728	116	63	43	33	27
^{16}N	0.78	0.78	0.78	0.77	0.77	0.76

Table 4

Concentration of Activity Induced In Air at Equilibrium (kBq m^{-3})

Under Specified Conditions† for a p(66)Be(49) Neutron Beam

NUCLIDE	Air Changes Per Hour					
	0	2	4	6	8	10
^{11}C	131	66	45	33	27	22
^{13}N	514	347	262	210	176	151
^{15}O	220	200	184	170	158	147
^{39}Cl	0.16	0.05	0.02	0.02	0.01	0.01
^{41}Ar	3.3	0.6	0.2	0.2	0.1	0.1
(^{16}N)*	260	260	260	260	250	250
TOTAL	1128	847	751	673	611	570
Time (min) to Decay to <370 kBq m^{-3}	9.4	3.1	1.3	0.6	0.3	0.2
Time (min) to Decay for I_pV/P X (1/2)	1.3	0.2	-	-	-	-

† Beam Volume: Trapezoidal, defining a 30x30 cm^2 field at 170 cm from source, 5 m long.
Room Volume = 200 m^3
Beam Current = 100μA

Table 5

Integrated Radionuclide Production in Body of

Standard Man from Neutrons in a p(66)Be(49) Beam.

NUCLIDE	Transformed Nuclei per Unit Activation Time (s^{-1} μA^{-1} m^{-3})	Activity per Unit Dose (MBq Gy^{-1} m^{-3})*
^{11}C	5.33 ± 0.15 E8	952 ± 27
^{13}N	6.65 ± 0.67 E7	243 ± 24
^{15}O	7.32 ± 0.39 E8	1.30 ± 0.07 E4
(^{12}B)**	4.2 ± 2.0 E8	4.5 ± 2.1 E7
(^{16}N)**	8.8 ± 5.9 E8	2.7 ± 1.8 E5

* Using a neutron dose rate per unit proton current of 3.2×10^{-4} Gy s^{-1} μA^{-1} at the target volume.

** Estimates, see text.

Table 6

Added Dose Due to Decay of Activity Induced in 10^{-3} m^3 (1ℓ) of Standard Man Uniformly Irradiated by a p(66)Be(49) Neutron Beam

Radionuclide	Added Dose (Gy per given Gy)		
	In Treatment Volume	Total Body	Outside Treatment Volume
^{11}C, ^{13}N, ^{15}O	4.8 E-4	9.8 E-6	2.5 E-6
^{12}B, ^{16}N	2.9 E-3	4.9 E-5	4.4 E-6
^{31}Si, ^{28}Al ^{30}P, ^{34}Cl ^{39}K	∿3 E-5	∿6 E-7	∿7 E-8
^{24}Na, ^{32}P, ^{38}Cl, ^{42}K, ^{49}Ca	∿2 E-6	∿5 E-8	∿9 E-9
TOTAL	3.4 E-3	5.9 E-5	7.0 E-6

*All radionuclides below dashed line are estimates. See text.

Figure Captions

Fig. 1. Calculated $^{12}C(n,2n)$ cross section as a function of energy.[6]

Fig. 2. Neutron energy spectra for the p(66)Be and p(41)Be beams.[11] Solid lines indicate reference spectra. Broken lines represent spectral variations for the p(41)Be beam using half, twice or ingnoring the expected contribution from the evaporation process. The data (open circles) are from Ref. 12.

Fig. 3. Graphite decay data with fit of ^{11}C decay curve plus background to data.

Fig. 4. Melamine decay data with fit of ^{13}N and ^{11}C decay curves plus background to data.

Fig. 5. Distilled water decay data with fit of ^{15}O, ^{13}N, and ^{11}C decay curves plus background to data.

Fig. 1

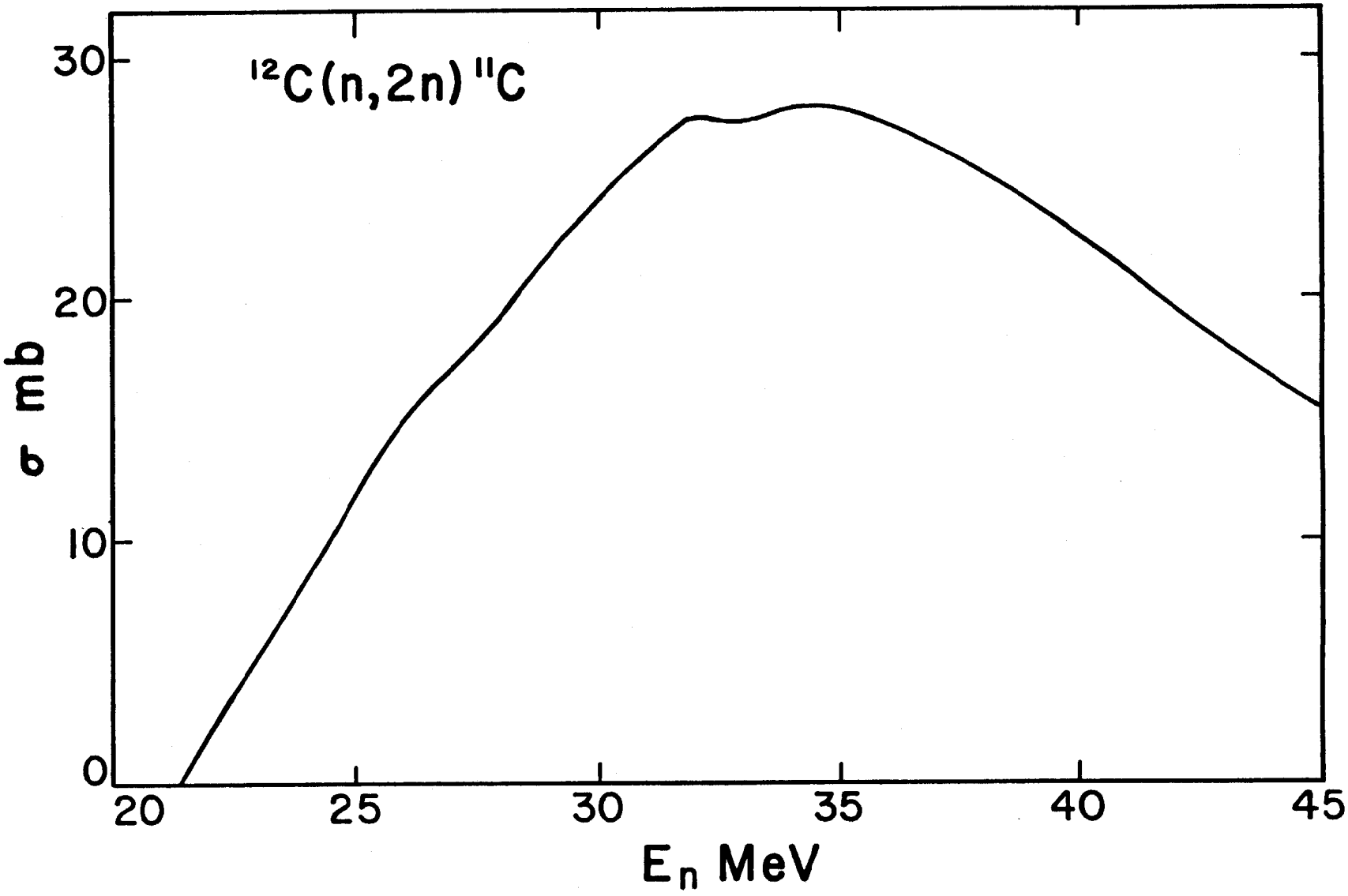

Fig. 2

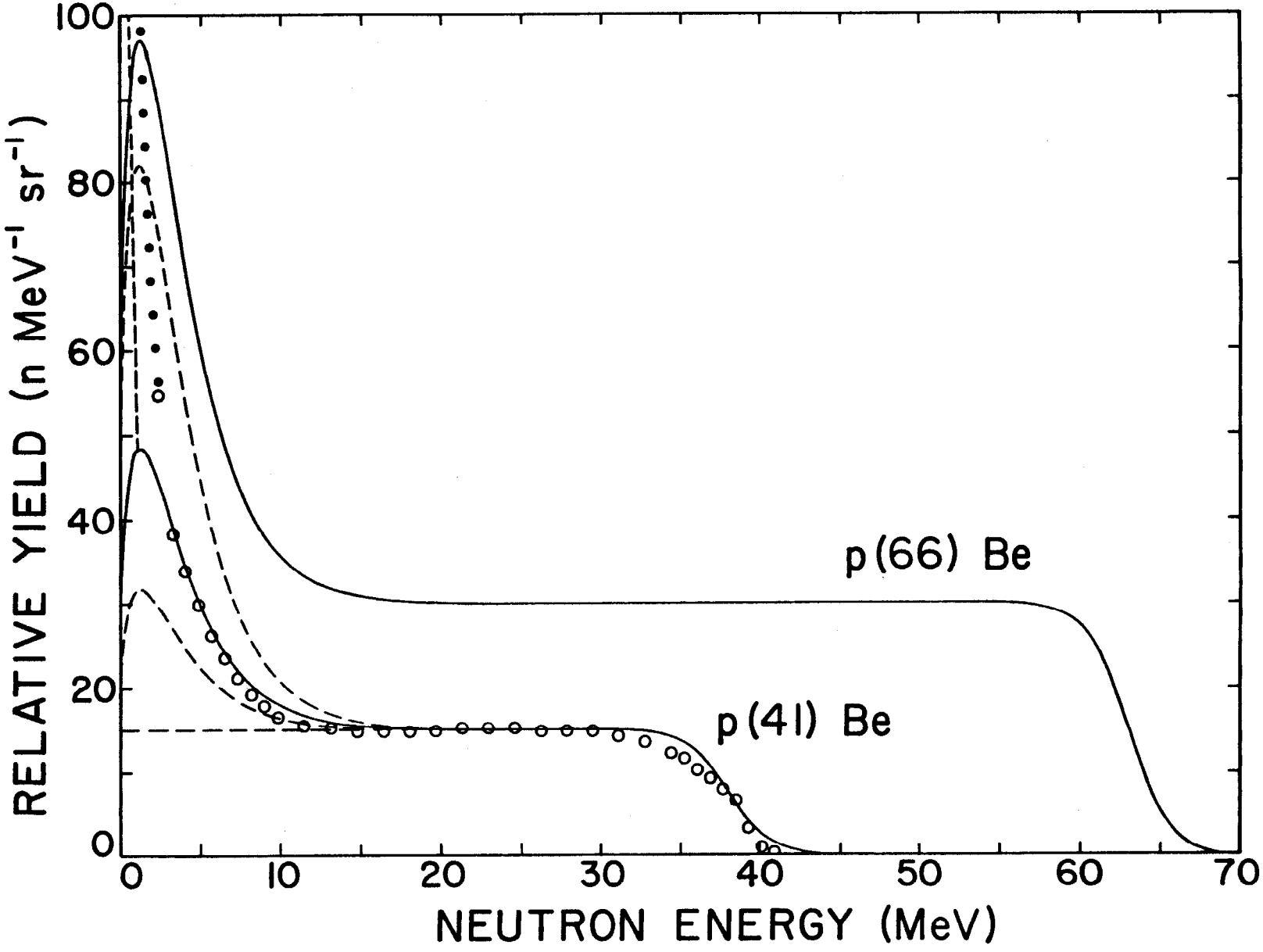
RELATIVE YIELD (n MeV^{-1} sr^{-1})
100
80
60
40
20
0
0
10
20
30
40
50
60
70
NEUTRON ENERGY (MeV)
p(66) Be
p(41) Be

Fig. 3

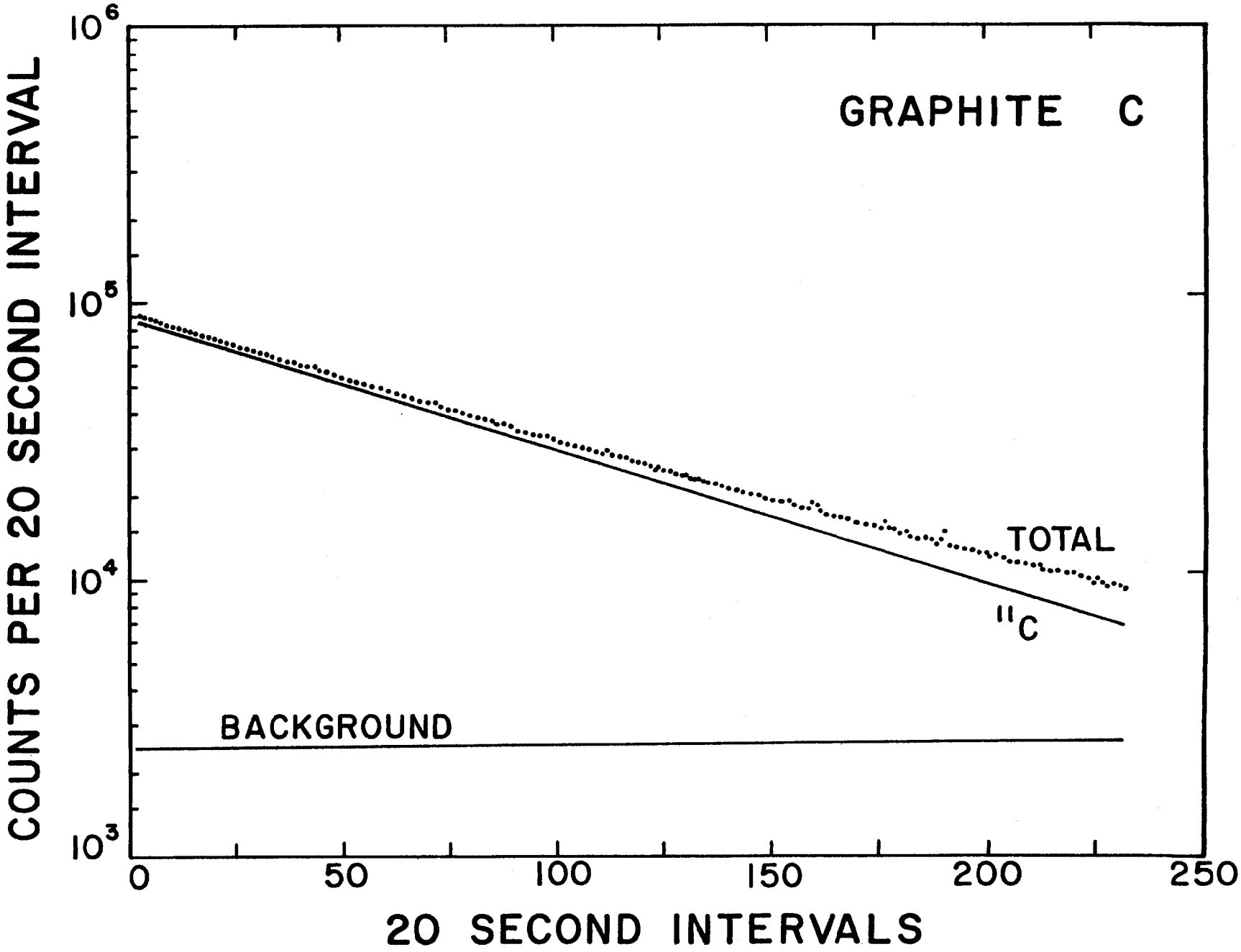
GRAPHITE C
TOTAL
^{11}C
BACKGROUND
COUNTS PER 20 SECOND INTERVAL
10^6
10^5
10^4
10^3
0
50
100
150
200
250
20 SECOND INTERVALS

Fig. 4

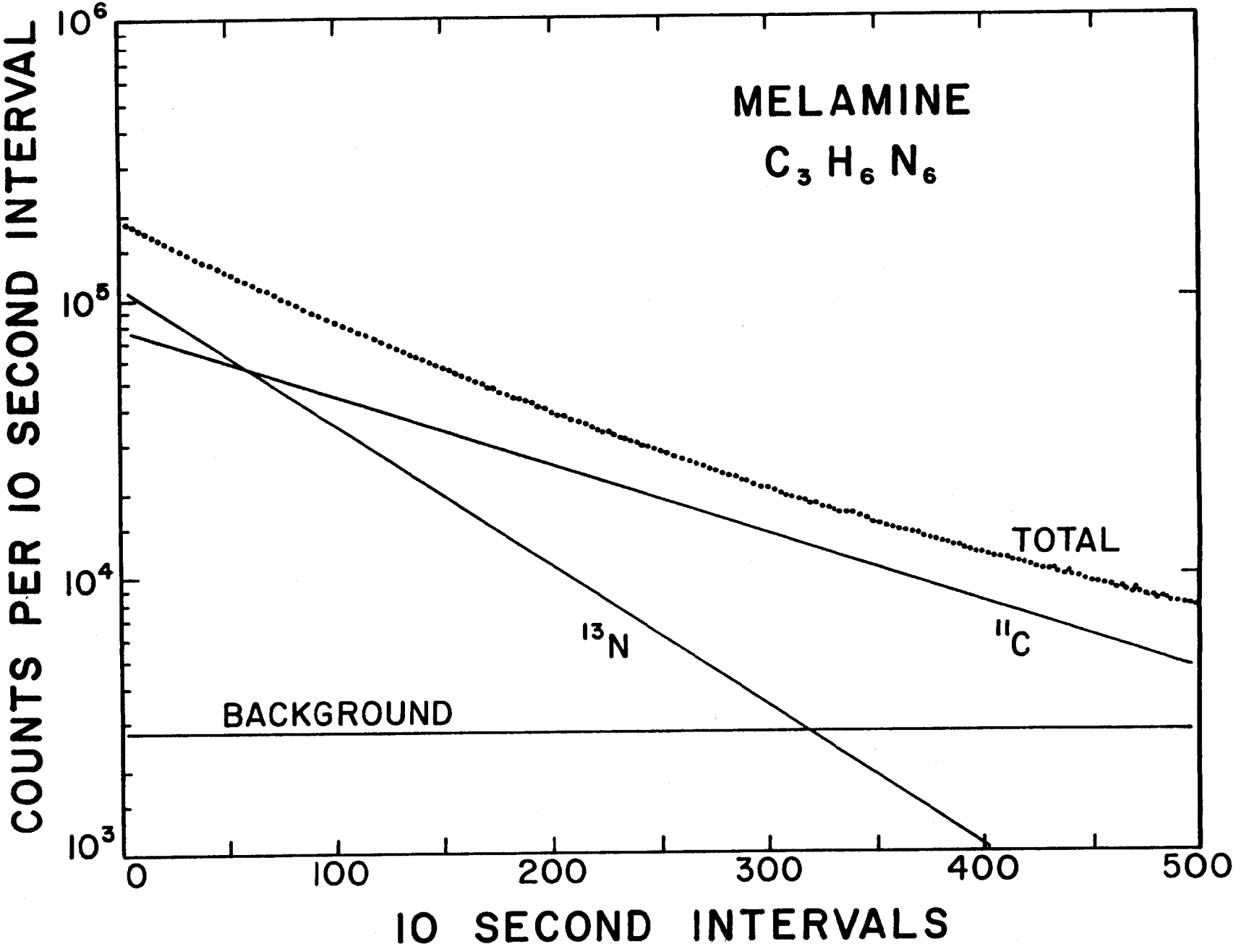
MELAMINE
$C_3 H_6 N_6$
TOTAL
^{11}C
^{13}N
BACKGROUND
COUNTS PER 10 SECOND INTERVAL
10^6
10^5
10^4
10^3
0
100
200
300
400
500
10 SECOND INTERVALS

Fig. 5

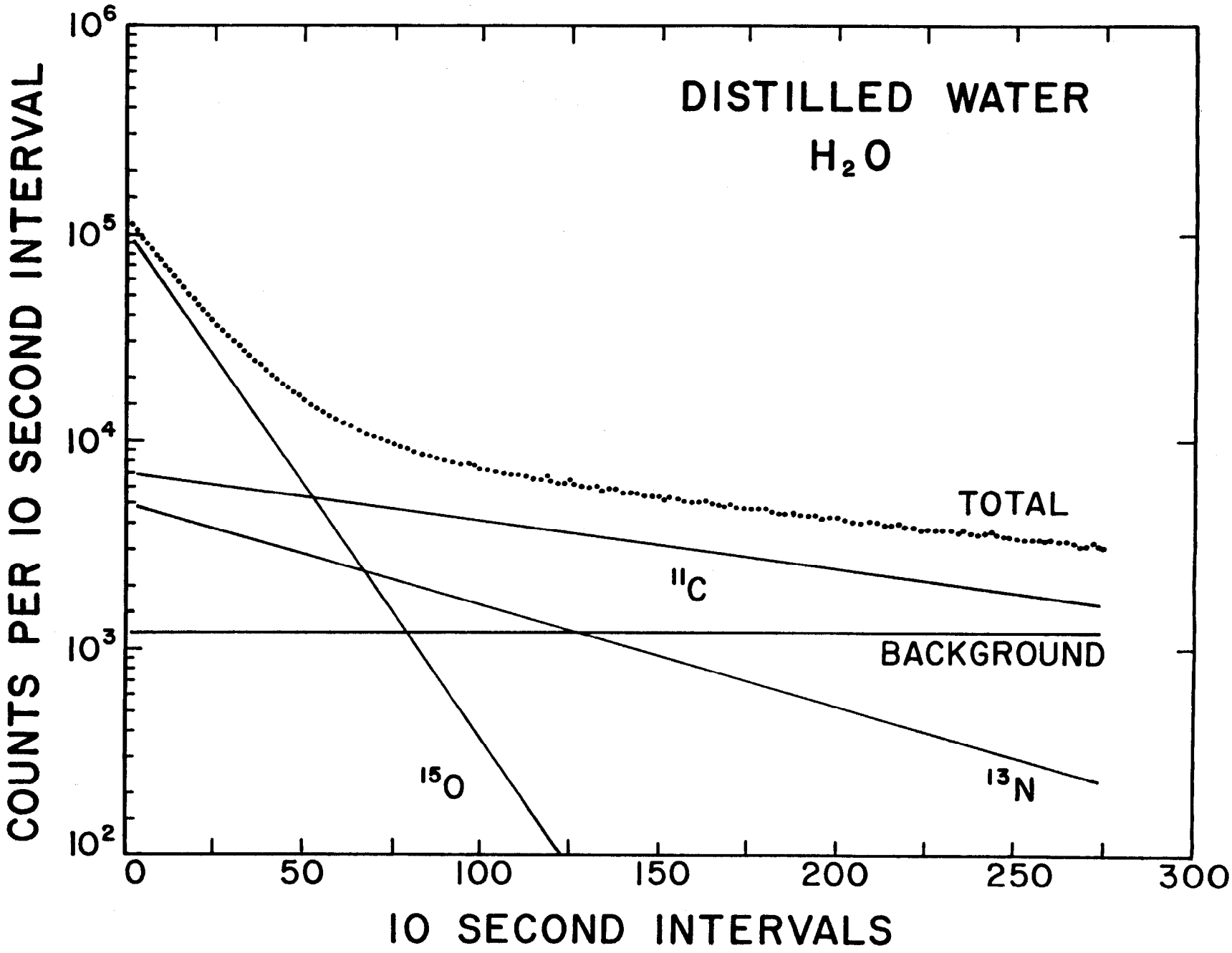
DISTILLED WATER
H_2O
TOTAL
^{11}C
BACKGROUND
^{15}O
^{13}N
COUNTS PER 10 SECOND INTERVAL
10^6
10^5
10^4
10^3
10^2
0
50
100
150
200
250
300
10 SECOND INTERVALS